Available online at www.sciencedirect.com

SciVerse ScienceDirect

journal homepage: www.elsevier.com/locate/watres

Fouling in reverse electrodialysis under natural conditions

David A. Vermaas [a,b], Damnearn Kunteng [c], Michel Saakes [a], Kitty Nijmeijer [b,*]

[a] Wetsus, Centre of Excellence for Sustainable Water Technology, Fac. of S&T, P.O. Box 1113, 8900 CC Leeuwarden, The Netherlands
[b] Membrane Science & Technology, University of Twente, P.O. Box 217, 7500 AE Enschede, The Netherlands
[c] REDstack, P.O. Box 199, 8600 AD Sneek, The Netherlands

ARTICLE INFO

Article history:
Received 13 September 2012
Received in revised form
22 November 2012
Accepted 27 November 2012
Available online 12 December 2012

Keywords:
Salinity gradient energy
Reverse electrodialysis
Fouling
Ion exchange membranes
Natural conditions
Field conditions

ABSTRACT

Renewable energy can be generated from mixing salt water and fresh water in reverse electrodialysis. The potential for energy generation from mixing seawater and river water is enormous. To investigate the effect of fouling when such natural feed waters are used, the performance of three different setups for reverse electrodialysis was evaluated for 25 days using seawater and river water as feed water, with no other (pre-)treatment than a 20 μm filter. Due to the absence of other anti-fouling treatments, a mixture of fouling is observed on the membranes, composed of remnants of diatoms, clay minerals, organic fouling and scaling. The fouling type was dependent on the different membrane types. The anion exchange membranes attract mainly diatoms and clay minerals, whereas scaling was only found on the cation exchange membranes. As a reference, plastic sheets without charge were used, which results in significant cleaner surfaces. Additionally, the setups without spacers in between the membranes (i.e. profiled membranes) appear significant less sensitive to fouling. This was quantified by the pressure drop over the feed waters and the power density obtained from the membrane piles. The pressure drop increases four times slower and the power density remains higher when profiled membranes are use instead of flat membranes with spacers. Although the obtained power density reduced with approximately 40% in the first day under these conditions, caused by organic fouling, several strategies are available to maintain a high power output using reverse electrodialysis.

1. Introduction

Salinity gradient power is a potentially large source for electricity generation. Energy can be extracted from mixing (salt) seawater and (fresh) river water, due to the increase in entropy. Considering the total global discharge of rivers to the sea, a theoretical power production of 2.4 TW is estimated Wick (1978), which is even larger than the present electricity consumption EIA (2010).

A technology to capture the power from salinity gradients is reverse electrodialysis (RED) Lacey (1980, Vermaas et al. (2011a). In reverse electrodialysis, an electrical potential difference is created when waters with different salinity are on either side of a membrane that allows the passage of only anions (anion exchange membrane, AEM) or only cations (cation exchange membrane, CEM). The potential difference, as generated by the salinity difference, generates an electrical current using electrodes and a reversible redox reaction. The

* Corresponding author. Tel.: +31 53 489 4185; fax: +31 53 489 4611.
E-mail address: d.c.nijmeijer@utwente.nl (K. Nijmeijer).
0043-1354/$ – see front matter © 2012 Elsevier Ltd. All rights reserved.
http://dx.doi.org/10.1016/j.watres.2012.11.053

electrical current can be used to power an electrical device. This process is illustrated in Fig. 1.

As an alternative technology, power from salinity gradients can be captured with pressure retarded osmosis (PRO) Norman (1974, Yip et al. (2011). Pressure retarded osmosis relies on water transport through semi-permeable membranes, which creates a pressure difference and generates a turbine. Regarding the fouling tendency, RED is expected less sensitive to clogging or fouling than PRO Post et al. (2007, Ramon et al. (2011, She et al. (2012), as in RED only ions pass the membranes, while water and additional colloids are retained the membrane and only flow along the membrane.

However, although the fouling issue in RED is expected to be less pronounced than in PRO, fouling may still be a problem. Previous research on fouling in RED is very limited. Post (2009) studied biological fouling and the effect of different strategies to prevent fouling and a subsequent increase in pressure drop due to this biofouling (e.g. reversing flow direction and switching feed waters), under accelerated biofouling conditions in a laboratory experiment. He concluded that the biofouling process could be slowed down when the feed water was interchanged and reversed in flow direction periodically, but fouling nevertheless occurred under the applied accelerated biofouling conditions. Only a setup without spacers did not show a significant pressure increase for 14 days under accelerated fouling conditions Post (2009). Also in other membrane technologies, such as reverse osmosis (RO), fouling is mostly concentrated on the feed water spacers Vrouwenvelder et al. (2009). A RED setup using profiled membranes instead of a design with spacers was recently presented Vermaas et al. (2011b). Such a spacerless setup is expected less sensitive to fouling.

The effects of other fouling types in RED, such as colloidal fouling and fouling with organic substances, were not studied before. The individual fouling types in electrodialysis are investigated in larger extent Katz (1979, Kim et al. (2011, Korngold et al. (1970, Lee et al. (2002, Lindstrand et al. (2000a, Lindstrand et al. (2000b), especially for anion exchange membranes, as they are most sensitive for organic and colloidal fouling Korngold et al. (1970, Lee et al. (2002, Lindstrand et al. (2000a, Lindstrand et al. (2000b). These fouling types are generally composed of large negatively charged molecules, and therefore attracted by the surface charge of the anion exchange membranes. All common fouling types in ED (organic, colloidal, biofouling, scaling) can be reduced by switching the electrical current direction frequently, for example by applying short electrical pulses Cifuentes-Araya et al. (2011, Lee et al. (2002) or by switching the feed waters Allison (1995, Katz (1979) (electrodialysis reversal, EDR). However, the fouling behavior in ED and EDR is expected to be different than that in RED. In ED and EDR, the process is opposite (concentrating the salt solution increases the risk of scaling), the typical intermembrane distances and current densities are much larger in ED/EDR and only one feed water type is used as inflow in that case.

Fouling studies for RED (but also for ED) under environmental conditions are sparse. Kjelstrup Ratjke et al. (1984) studied the power density obtained from a RED stack with spacers for 180 days, fed with natural seawater and artificial river water. They concluded that the power density was decreased by 67% after 180 days of operation, due to biological fouling Kjelstrup Ratjke et al. (1984). The pressure drop between the inlet and outlet of the feed water (which is a measure for the occurrence of fouling) was not reported. To our best knowledge, no research has been published so far, in which seawater and river water both from natural sources was used.

This research presents, for the first time, the fouling behavior of RED stacks that are operated for 25 days without cleaning and supplied by natural seawater and river water. The goal of this research is to characterize the typical fouling types in RED and the effect on the obtained power density and the pressure drop for pumping the feed waters. This research aims to indicate what fouling type limits the performance of RED, rather than focusing on a single controlled type of fouling. After a brief review of the expected influences of fouling in RED, an experiment is described and presented, where three different stack designs were fed by natural seawater and river water. One stack contained flat cation and anion exchange membranes with spacers in between, a second stack was spacerless using profiled cation and anion exchange membranes, and a third stack was spacerless using profiled (non-conductive and non-charged) plastic sheets, to show the effect of membrane charge. The differences in fouling behavior observed experimentally also show the directions for effective anti-fouling strategies.

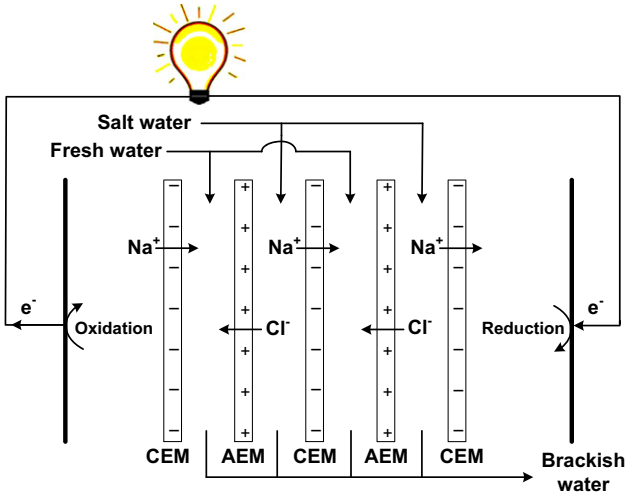

Fig. 1 – Principle of reverse electrodialysis (RED). The salt water and fresh water flow alternately along cation exchange membranes (CEM) and anion exchange membranes (AEM). A (reversible) redox reaction (in an electrolyte that can be circulated) converts the ionic current into an electrical current.

2. Theory

To distinguish the effects of fouling and the effects that can be due to this specific location and this specific experimental setup (such as salinity, temperature, flow rate), the performance of the RED stacks is compared to theoretical values that would be expected when no fouling would occur. These

expected theoretical equivalents can be deduced from laboratory experiments as published in previous research Vermaas et al. (2011a, b). Based on these experimental data, an analytical model was developed for realistic estimates of the open circuit voltage (OCV), resistance, power and pressure drop Vermaas et al. (2012). A brief description of this analytical model is given here.

2.1. OCV

The theoretical voltage that is created by the salinity difference over an ion exchange membrane is given by the Nernst equation. Corrected for the apparent mean permselectivity α of the ion exchange membranes, the voltage over N_m membranes can be calculated as:

$$E_{OCV} = \alpha \cdot N_m \cdot \frac{R \cdot T}{n \cdot F} \cdot \ln\left(\frac{\gamma_{sea} \cdot c_{sea}}{\gamma_{river} \cdot c_{river}}\right) \quad (1)$$

In which R is the universal gas constant (8.314 J/(mol K)), T is the absolute temperature (K), F is the Faraday constant (96485 C/mol), n is the valence of the ion species (−), γ is the activity coefficient of the salt species (−) and c is the concentration of the salt (mol/liter). The subscripts *sea* and *river* indicate seawater or river water, respectively.

Previous research showed that the apparent permselectivity is highest for membranes that have a high charge density (i.e. fixed charge in the membrane per volume of absorbed water) Długołęcki et al. (2008). Dissolved charged foulants, such as organic fouling, can counterbalance the fixed charge groups in the membrane, and reduce the apparent membrane permselectivity, which is observed before in electrodialysis Grebenyuk et al. (1998).

2.2. Electrical resistance

The electrical resistance of a RED stack is composed of the ohmic resistance (dependent on the conductivity of the membranes and feed waters) and a non-ohmic resistance. The non-ohmic resistance slowly develops when an electrical current is set and the ions are transferred from the seawater to the river water side. The ion transfer reduces the salinity difference and as a consequence reduces the electromotive force, which can be interpreted as a (non-ohmic) resistance when divided by the electrical current. The total electrical resistance of a RED stack is the sum of the described components (all in Ω cm^2):

$$R_{total} = R_{ohmic} + R_{non-ohmic} \quad (2)$$

The experiments can reveal both R_{ohmic} (from the instantaneous voltage drop at a current interruption) and the sum of all components R_{total} (from the stationary voltages) directly Vermaas et al. (2011a). The resistances in eq. (2) can also be estimated theoretically, based on the membrane specifications, water conductivity, water temperature, flow rate and cell dimensions Vermaas et al. (2012).

The resistance increases when membranes are fouled, due to two mechanisms. First, dissolved charged foulants, such as organic fouling, can counterbalance charged groups in the membrane, and therefore increase the ohmic resistance of the membrane Grebenyuk et al. (1998, Lindstrand et al. (2000a, Lindstrand et al. (2000b). Anion exchange membranes (AEMs) are more sensitive for this type of fouling than cation exchange membranes (CEMs) Korngold et al. (1970, Lindstrand et al. (2000a, Lindstrand et al. (2000b) because organic salts are often composed of a large anion ('poisoning' the AEM) and a small cation (which can pass the CEM). Additionally, research in ED showed that colloids adhered to the membranes increase the thickness of the concentration boundary layer, and therefore increase the non-ohmic resistance Korngold et al. (1970).

2.3. Power density

The power density that is generated by a RED stack equals the product of the voltage and the electrical current, divided by the membrane area. The current can be chosen, based on the external load that is connected. A small current yields a high voltage and vice versa. The maximum obtainable power density (W/m^2) can be calculated by Vermaas et al. (2011a):

$$P = \frac{E_{OCV}^2}{4 \cdot N_m \cdot R_{total}} \quad (3)$$

A part of the produced energy is consumed by pumping the feed water through the stack. When this part is subtracted, the net power density is obtained, given by:

$$P_{net} = \frac{E_{OCV}^2}{4 \cdot N_m \cdot R_{total}} - \frac{\Delta p_{sea} \cdot Q_{sea} + \Delta p_{river} \cdot Q_{river}}{N_m \cdot A} \quad (4)$$

in which Δp is the pressure drop (Pa) over the inlet and outlet of the feed water, Q is the flow rate (m^3/s) of the feed water and A is the area of one membrane (m^2).

Obviously, the presence of colloidal fouling and biofouling will increase the pressure drop over the feed water channels Post (2009), and therefore reduce the net power density.

3. Experimental setup

Three stacks were built, each containing 11 membranes that create 5 compartments for seawater and 5 compartments for river water. The first stack was built with flat ion exchange membranes and spacers in between. The second stack was spacerless, using profiled ion exchange membranes Vermaas et al. (2011b). The third stack was also spacerless, but used profiled plastic sheets that are not ion-conductive. This enables to test the effect of spacers on fouling, but also to test the effect of membrane surface charge on fouling. The specifications of these stacks are given in Table 1.

The electrode dimensions and the effective membrane area of each membrane was 10 × 10 cm^2. The profiled membranes and the profiled plastic sheets were created by thermal pressing for 10 min at 140 °C and 200 bar. The resulting profiled membranes and profiled plastics had ridge-structured corrugations of 200 μm wide in a parallel orientation at every 1 mm. More details, such as the geometry of the profiled membranes and the spacers, are described in previous research Vermaas et al. (2011b). The stacks were assembled and the membranes were brought in equilibrium for 24 h in artificial seawater (0.5 M NaCl) and river water (0.017 M NaCl) before use.

Table 1 – Specifications of the 3 RED stacks as used in this research.

	Stack 1	Stack 2	Stack 3
Membrane material	Ralex CMH/AMH	Ralex CMH/AMH	LD-PE
Membrane surface	Flat	Profiled	Profiled
Surface contact angle	n/a	58 ± 3°	98 ± 12°
Compartment support	Spacer (Sefar Nitex 07-300/46)	Membrane profile	Plastic profile
Intermembrane distance	240 ± 10 μm	240 ± 10 μm	200 ± 10 μm

All experiments were conducted at the Wetsalt demo site in Harlingen, The Netherlands, during summer, from August 9th to September 2nd 2011. All stacks were fed continuously with natural seawater and natural fresh water, at a flow rate of 100 ml/min (unless stated otherwise). Fresh water was obtained from a nearby canal (Van Harinxmakanaal) and salt water was obtained from the nearby harbor in the Wadden Sea. The water was pre-filtered through a series of microfilters, in which the final filter had a median diameter of 20 μm. No additional fouling prevention was applied. The feed water was not switched, nor reversed.

The pressure difference over the inlet and outlet of each feed water channel (for each stack) was measured with six differential pressure meters (Endress + Hauser, Deltabar S, Germany). The pressure differences were recorded every 30 s in a data logger (Endress + Hauser, Ecograph T, Germany).

The conductivity and temperature of the influent and effluent were monitored (ProMinent, Dulcometer, Germany) and recorded every 30 s (LabView 7.1, National Instruments, United States). Samples of the influent were taken three times during the experiment and the chemical composition of the water was analyzed using ion chromatography (IC) and inductively coupled plasma (ICP).

The OCV, the (ohmic and total) electrical resistance and the power density of the stack with spacers and the stack with profiled membranes was measured three times a week, each time in duplicate (or more), using chronopotentiometry (Iviumstat, Ivium Technologies, The Netherlands). To facilitate an electrical current, the electrodes (Ti mesh, coated with Ir/Ru) were supplied with an electrode rinse solution of 0.25 M NaCl. Two reference electrodes were installed at each stack, one connected to each electrode compartment. Hence, the voltage over the membrane stack only was measured, excluding the overpotential of the electrodes.

At the end of the experiment, the stacks were opened and fouled membrane samples were analyzed using a scanning electron microscope (SEM), Energy Dispersive X-ray spectroscopy (EDX) and X-Ray diffraction (XRD).

4. Results

To show the effect of fouling in this experiment, the feed water properties are shown first, followed by a visual and microscope inspection of the fouled samples. Later, the effect of the fouling on the performance during the experiments is shown, quantified by the pressure drop, obtained power density, apparent permselectivity and ohmic resistance of the reverse electrodialysis stacks.

4.1. *Feed water properties and effect of multivalent ions*

The feed water is characterized by the salinity, temperature, ion composition and total organic carbon (TOC) as given in Table 2. The standard deviations indicate the temporal variability of each parameter. The fluctuations in salinity and temperature emphasize that the actually measured power density must be normalized to theoretical equivalents (eqs. (1)–(3)) in order to distinguish the effects of fouling and the effects of changes in salinity and temperature. Although the relatively low salinity of the seawater (Wadden sea) will yield low absolute values for the power density compared to most laboratory research Ramon et al. (2011), Vermaas et al. (2011a, b), the normalized values will be representative for a wider range of feed water concentrations.

As typically for natural seawater and river water, the species Na^+ and Cl^- have the largest concentrations in both streams. Nevertheless, the presence of the multivalent ions (Ca^{2+}, Mg^{2+}, SO_4^{2-}), in approximately the same relative amount in both feed waters, will significantly reduce the produced voltage Post et al. (2009). When comparing solutions with monovalent ions only to solutions with multivalent ions only, the salinity gradient in monovalent ions would produce twice the voltage that multivalent ions would generate (eq. (1)). A mixture of monovalent and multivalent ions gives a more complex situation. Because the voltage generated by the salinity gradient of the monovalent ions is larger than the voltage that follows from the salinity gradient of the

Table 2 – Salinity, temperature and composition of the natural seawater and river water that were used for this research.

	Salinity (mM)	Temperature (°C)	Cations (mM)	Anions (mM)	Other (mg/L)
Seawater	280 ± 10	19 ± 2	Na^+: 202 ± 10 Ca^{2+}: 7 ± 1 Mg^{2+}: 28 ± 2	Cl^-: 242 ± 10 SO_4^{2-}: 11 ± 0	PO_4^{3-}: 2.8 ± 0.2 TOC: 10 ± 5
River water	38 ± 5	19 ± 3	Na^+: 38.7 ± 3.0 Ca^{2+}: 2.2 ± 0.9 Mg^{2+}: 3.3 ± 0.9	Cl^-: 43.9 ± 2.5 SO_4^{2-}: 2.3 ± 0.1	PO_4^{4-}: <0.5 ± 0.1 TOC: 18 ± 6

multivalent ions, two monovalent ions are exchanged for one multivalent ion to restore the inequality in the voltages that follows from the salinity gradients of monovalent and multivalent ions. In other words, a divalent ion can be drawn back to the saline compartment and exchanged for two monovalent ions Post et al. (2009), without a net electrical current. Consequently, the salinity gradient for monovalent ions will decrease and the produced voltage will decrease. Therefore, the addition of multivalent ions to a solution with monovalent ions works counterproductive for reverse electrodialysis. Based on the concentrations in Table 2, and assuming that multivalent ions exchange for monovalent ions until their corresponding voltages are balanced, the presence of multivalent ions decreases the produced voltage by approximately 7%. In addition, the membrane selectivity is lower for multivalent ions, but this effect is insignificant for the voltage when using homogeneous membranes.

In addition, the multivalent ions have a minor effect on the electrical resistance. The resistance of the water compartments is decreased by the presence of multivalent ions on one hand, but the electrical resistance of the membranes increases, compared to monovalent ions with the same concentration Post et al. (2009). As a consequence, the total resistance can increase or decrease due to the presence of multivalent ions, dependent on the contributions of the feed waters and membranes in the total stack resistance.

4.2. *Visual and microscopic inspection*

After 25 days of operation, the membranes and spacers of all stacks are investigated visually and by SEM. The anion exchange membranes (AEMs) are colored brown-red (originally beige), while the cation exchange membranes (CEMs) and the profiled plastics preserve their original beige color. The brown-red color of the AEMs indicates that negatively charged molecules, such as humic acids, are absorbed on the AEMs.

In addition to the color of the membrane, a grey-brown material filled up a part of the porous spacers (both for seawater and river water) and the channels in the profiled AEMs. The distribution of this fouling is not equal, but concentrates at more or less random locations over the spacer or membrane. The profiled CEMs and the profiled plastics are covered with less of this grey-brown deposition, except for the part of the membranes close to the inlet and outlet of the feed water. The profiled plastics in contact with the seawater are optically least fouled; more than 95% of the area of their sheets are visually clean.

The fouled membrane/plastic samples from all stacks are inspected with SEM and representative images are shown in Fig. 2. These images show that all samples, except for the profiled plastic in seawater, are covered with a mixture of deposits. Remnants of diatoms are found, most densely present at the AEMs in river water samples. The river water is probably the largest source of these remnants of diatoms, and these diatoms are attracted to the AEMs because of the negative charge on the silica skeleton of the diatoms Sumper (2002). Apart from a few green algae and bacteria (at the profiled plastic in seawater), no intact organisms are observed.

The CEMs in seawater show spherical structures, most pronounced at the profiled CEM in seawater, possibly growing mineral crystals. The remaining part of the deposit is

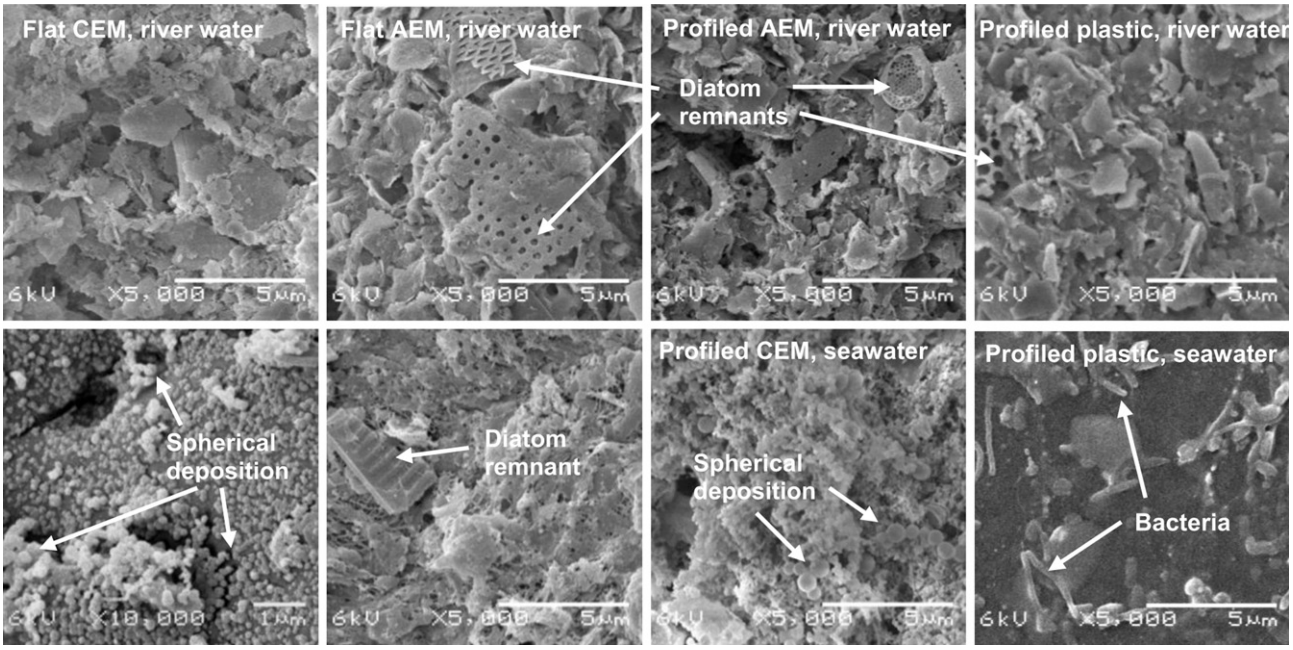

Fig. 2 – SEM images of cation and anion exchange membranes (CEMs and AEMs) and profiled plastics. The images in the upper row were in contact with river water, whereas the images in the lower row where in contact with seawater. The four images at the left side are obtained from flat membranes (stack 1, river water side and seawater side), the four images at the right side are obtained from profiled membranes (stack 2) and profiled plastics (stack 3). Most images were saved at a magnification of 5000×, only the flat CEM in contact with seawater was saved at 10,000×, to see the spherical deposition. Remnants of diatoms, bacteria and spherical deposition are indicated by arrows.

comprised of unorganized fragments of typically 1 μm size. This was observed for both the profiled membranes and the flat membranes. The composition of these fragments and crystals is investigated using Energy Dispersive X-ray spectroscopy (EDX) for all samples. The elements that appear in highest quantities in the samples from the flat membranes of stack 1 (both seawater and river water side) are listed in Table 3.

The relatively high carbon content in the EDX-results is the result of the polymer structure of the membrane, which contains significant amounts of carbon. The higher standard deviation in carbon content for the CEMs is because the fouling layer is thinner and sometimes does not cover the full area in case of CEMs. The concentration of calcium and phosphorus are typically higher according to the EDX-results (Table 3) on the cation exchange membranes at the seawater side, especially when the image was zoomed to the spherical deposition in this fouling layer (Fig. 2, middle images at lower row). Calciumphosphates can be precipitated as a consequence of increased concentrations due to the exchange of multivalent ions for monovalent substitutes. This ion exchange causes a higher concentration of multivalent ions (such as calcium and phosphate) in the seawater compartment. This may be more pronounced visible at the CEM than at the AEM, because the fouling in the AEM is dominated by other colloids. In electrodialysis, scaling is also observed more pronounced at CEMs than at AEMs Korngold et al. (1970).

The fouling layer at the anion exchange membranes shows higher contents of Si and O than at the cation exchange membranes (Table 3), indicating silica components. To distinguish whether this silica originates from the diatoms or from non-organic substances (e.g. clay minerals), XRD was performed. Some samples show hardly any peaks in the XRD-spectrum, while other samples show sharp peaks which are most pronounced at twice the diffraction angle (2θ) of 26.8, 31.8, 35.0, 45.6, and 56.6°. The peaks at 26.8, 35.0 and 45.6° correspond to the clay mineral muscovite, composed of $KAl_2(Si_3Al)O_{10}(OH)_2$ RRUFF (2012). This corresponds to the EDX-results qualitatively, where the contents of aluminum and potassium are significantly higher at AEMs than at CEMs. However, the ratio between aluminum, silicon and oxygen from Table 3 does not match the ratio of the elements in muscovite. The content of silicon is relatively higher. Moreover, some samples did not show these peaks. In conclusion, the fouling layer can be considered as a mixture of clay minerals (e.g. muscovite) and amorphous silica from diatoms.

Although this specific clay mineral is dependent on the exact feed water content, the accumulation of clay minerals and diatoms to the AEMs is expected in general, due to the net negative charge on these particles. Both the mineral muscovite and the silica shell of diatoms carry a net negative charge, which explains their presence at the AEMs and not at the CEMs. Similar observations are done in electrodialysis Korngold et al. (1970, Lee et al. (2002).

The rather clean plastic sheets from stack 3 show that the charge of the membrane is important in attracting fouling. Moreover, the non-conductive plastic sheets from stack 3 disable ion exchange, and therefore the scaling as seen on the CEMs is not present on the plastic sheets.

4.3. *Pressure drop*

Time series for the pressure drop over the inlet and outlet of the feed waters, for all three stacks, are presented in Fig. 3.

The pressure drop in the stack with spacers increased rapidly to the maximum value that the feed water pumps could produce (~1.5 bar). Since the pumps could not produce an even higher pressure on the feed water, the pressure for the stack with spacers remained at its maximum value, but the flow rate for the stack with spacers slowly decreased after 5 days, to only 10% of its original value after 25 days.

For the stack with profiled membranes, the pressure drop increased much slower than for the stack with spacers. The pressure drop increased to 1.5 bar in approximately 20 days after the start of the experiment (Fig. 3). The slower increase in pressure in the stack with profiled membranes, compared to the stack with spacers, can be explained by the absence of woven spacer structure. The woven spacer structure, with its crosswise filaments and knits, leaves only small openings for the feed water flow and creates regions with wakes. Colloids are easily trapped in the small openings, which increase the pressure drop in the stack with spacers. The smooth, parallel channels that are created by the profiled membrane give less opportunity for colloids to attach, and consequently resulting in a less steep increase of the pressure drop.

The pressure drop over the feed water in the stack with profiled plastic increased even slower; the pressure drop increased to 500 mbar after 23 days (Fig. 3). As shown in Fig. 2,

Table 3 – EDX of CEM and AEM (seawater and river water side) from the stack with spacers (stack 1), in atom percentage. The composition of the fouling in stack 2 is similar. The EDX-results of the samples from stack 3 are dominated by the carbon content of the plastic, because the fouling layer was insufficient to cover the plastic polymer fully. The values with standard deviation are measured in triplicate, the other values are measured once.

	Flat CEM (stack 1), seawater side	Flat CEM (stack 1), river water side	Flat AEM (stack 1), seawater side	Flat AEM (stack 1), river water side
Carbon (%)	42 ± 28	22	45	51 ± 2
Oxygen (%)	36 ± 18	53	35	31 ± 1
Silicon (%)	4 ± 1	6	7	8 ± 1
Potassium (%)	0 ± 0	1	1	1 ± 0
Calcium (%)	6 ± 3	4	1	0 ± 0
Aluminum (%)	1 ± 0	4	2	3 ± 0
Phosphorus (%)	7 ± 4	5	2	1 ± 0

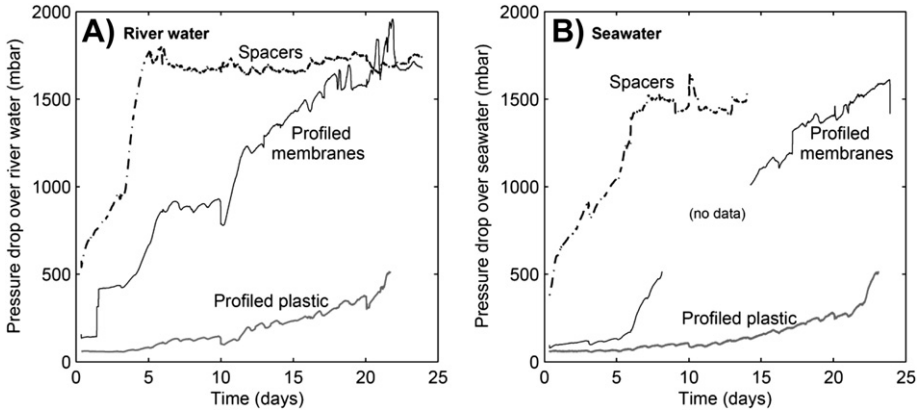

Fig. 3 – Pressure drop over the river water (A) and over the seawater (B) compartments, plotted against the time after the start of the experiment. A part of the series for the pressure drop over the seawater is not recorded, because the pressure meter that was used for profiled membranes was out of range. The pressure meter for the stack with spacers is used for the stack with profiled membranes from day 14 on.

the uncharged plastic sheets did not attract (charged) colloids and therefore the pressure drop remains lowest in the stack with profiled plastic.

The pressure drop in the stack with profiled plastic was also lowest from the start of the experiment, although the intermembrane distance was slightly smaller than for the other two stacks. The hydrophobic property (Table 1) of the uncharged plastic may cause a slip of the hydrodynamic boundary layer of the feed water, whereas the water flow over the hydrophilic membranes has a no-slip boundary condition. Although the hydrophobic 'membrane' surface reduces the pressure drop, it may be unfavorable for ion transport. Since the profiled plastic is non-conductive, this could not be tested in this experiment.

The pressure drop does not increase monotonically, but decreases at some days, for example at day 10 and day 16 (Fig. 3). At these days, the 20 μm filters were changed and the pumps were stopped shortly. Although the pumps were only stopped for approximately 5 min, the pressure drop of the profiled membranes remained at a lower value for about 1 day. The small pressure shock, that is created by stopping and starting the pumps, clears up the colloids that block a part of the compartment. This effect is most pronounced visible for the stack with profiled membranes (Fig. 3), because the colloids are harder to remove from the knitted structure of the spacers. This suggests that a pulsating flow, which is used as anti-fouling strategy in other applications Blel et al. (2009), is effective to reduce the pressure drop in a stack with profiled membranes even more.

4.4. *Power density*

The apparent permselectivity, resistance, and power density were normalized using eqs. (1)–(4) and the actual temperature, salinity and flow rate, to account for the changes in these parameters during the experiment. In addition, assumptions are made to obtain the normalized values. The average apparent permselectivity of the Ralex membranes, using monovalent ions, is assumed 92% Vermaas et al. (2011b). The presence of multivalent ions reduces the open circuit voltage by another 7%, which yields 85% of the voltage that would be obtained with perfectly selective membranes and if monovalent ions only would be present. We assume that the response time and apparent membrane selectivity for multivalent ions is similar for the membranes in this research as for homogeneous membranes Post et al. (2009). The average membrane resistance of all membranes is assumed 5.5 Ω cm^2 Vermaas et al. (2011b). The spacer shadow effect is modeled using a spacer mask factor of 0.5 for spacers (50% open area) Vermaas et al. (2012) and 0.2 for the profiled membranes (20% of the area covered by ridges Vermaas et al. (2011b)). The conductivity of the feed water compartments is corrected for the (spacer) porosity Vermaas et al. (2012), which is assumed 75% for spacers and 80% for the profiled membranes (20% occupied with ridges).

The normalized power density, as function of the number of days of operation, is shown in Fig. 4. The power density at the very beginning is close to the expected value (100%), but decreases by more than 40% in the first day and then remains more or less constant, with a slow decrease at the end of the experiment for the stack with profiled membranes. The stack with profiled membranes performs relatively better than the stack with spacers. In absolute values, the difference between the stacks is even larger (110–140 mW/m^2 for profiled membranes versus 50–80 mW/m^2 for the stack with spacers). The normalization of the power density, considering the lower flow rate in the stack with spacers after the fifth day, reduces the relative difference.

The decrease in power density is much faster than the increase in pressure drop (Fig. 3), which suggests that the decrease in power density is caused by another mechanism than that for the increase in pressure drop. Also the presence of multivalent ions cannot explain the decrease in power density, since the theoretical voltage includes the effect of multivalent ions. The decrease in power density could be caused by organic fouling, preferential channeling or a very thin layer of deposits that isolates the ion-conductive membranes. To distinguish these effects, the open circuit

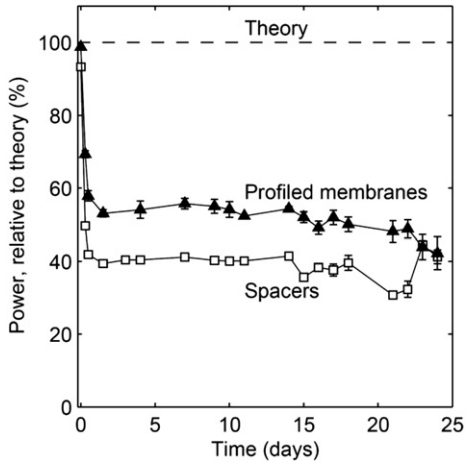

Fig. 4 – Obtained power density as function of the number of days after the start of the experiment, for a stack with spacers (open symbols) and a stack with profiled membranes (filled symbols).

voltage (i.e. apparent permselectivity) and ohmic resistance are analyzed.

4.5. *Permselectivity and resistance*

The apparent permselectivity and normalized ohmic resistance, as derived from the stacks with spacers and the stack with profiled membranes, are shown in Fig. 5.

The apparent permselectivity decreases sharply (by approximately 10%) and the electrical resistance increases rapidly (by 40%–70%) during the first day of the experiment. Although the relative increase in the resistance is larger than the decrease in apparent permselectivity, both have a major effect on the power density, since the power density is dependent on the apparent permselectivity squared (eq. (3)). The significant decrease in apparent permselectivity and increase in ohmic resistance suggests that organic fouling plays an important role. These charged molecules are large in comparison to ions and will be trapped in the surface layer of the ion exchange membranes where they counterbalance the effective surface charge of the membranes. As a consequence, the charge density that is available for ion transport decreases. This causes the reduced apparent permselectivity Długołęcki et al. (2008, Grebenyuk et al. (1998) and increased ohmic resistance Grebenyuk et al. (1998, Korngold et al. (1970, Lindstrand et al. (2000b). Preferential channeling or a very thin layer of deposits on the membranes could show an increase in electrical resistance, but does not explain the decrease in permselectivity.

The changes in permselectivity and ohmic resistance are larger in the stack with spacers compared to the stack with profiled membranes, probably because organic fouling intensifies in the case with spacers, due to the relatively large membrane area that is covered by non-conductive spacers. The larger (local) current density increases the rate and the degree of organic fouling Lindstrand et al. (2000a). The same would apply for RED stacks that operate at a higher current density, for example when homogeneous membranes are used that have a lower electrical resistance than the membranes used in this research.

5. Possible anti-fouling strategies

The present research shows that fouling quickly reduces the power density if no anti-fouling strategies (other than a microfilter) are applied. However, several options to reduce fouling and maintain a sufficiently high power density are available. The decrease in power density occurs faster than the increase in pressure drop. This suggests that strategies against non-colloidal fouling are required to maintain a high power density. In electrodialysis, an effective strategy to reduce the effect of fouling is to periodically switch the electrical current direction, by means of switching the feed waters. For electrodialysis, this strategy is called electrodialysis reversal (EDR). This strategy appeared effective to reduce organic fouling, charged colloids Allison (1995, Katz (1979) and scaling Grebenyuk and Grebenyuk (2002) in EDR, as well as to reduce possible biofouling in RED Post (2009). This strategy will be most effective for a stack with profiled membranes,

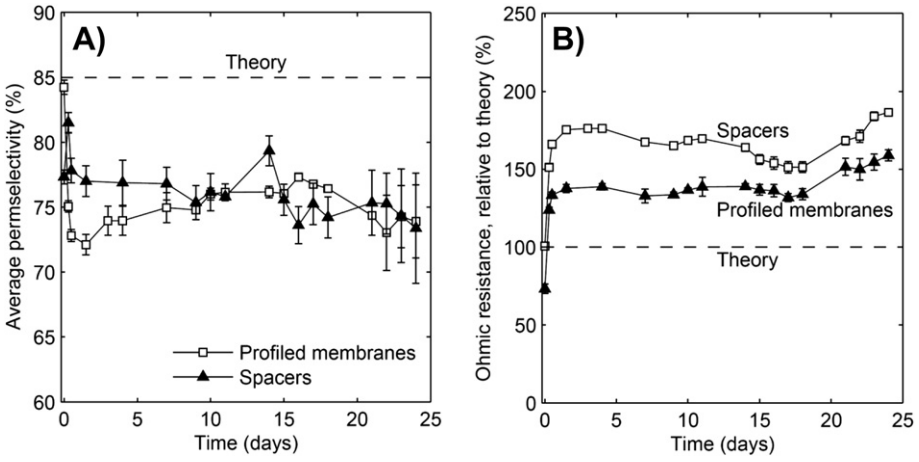

Fig. 5 – Apparent permselectivity (A) and ohmic resistance relative to the theoretical ohmic resistance (B) as function of the time after the start of the experiment.

since this research indicated that disturbances are more effective in removing colloids for a stack with profiled membranes, compared to a stack with spacers. Alternatively, short electrical pulses in the opposite direction reduce the effect of humate fouling in ED Cifuentes-Araya et al. (2011, Lee et al. (2002), and may also be effective for maintaining a high power density is RED. As a third option, a chemically modified membrane surface, using for example high molecular mass surfactants, make the anion exchange membranes less sensitive for organic fouling Grebenyuk et al. (1998). These surfactants have a fixed negative charge, that repels large organic anions from the anion exchange membrane, while the selectivity and conductivity of the membrane where only slightly affected Grebenyuk et al. (1998). Adding a surfactant with a fixed charge opposite to the fixed charge in the membrane also creates selectivity for monovalent ions Post et al. (2009), in a way similar to the commercial monovalent selective membrane Neosepta CMS, for example. The use of monovalent selective membranes reduces the exchange of multivalent ions for monovalent ions and the corresponding voltage decrease Post et al. (2009).

6. Conclusions

Reverse electrodialysis stacks are successfully used to generate electricity from mixing natural seawater and natural river water. When no anti-fouling strategies are applied (other than a 20 μm filter for the feed water), a mixture of fouling on the membranes and spacers increases the pressure drop over the feed water and reduces the obtained power density. When spacers are substituted for profiled membranes, the effects of fouling are reduced; the pressure drop increased four times slower and the power density remained relatively higher. Such spacerless stacks using profiled membranes are regarded less sensitive to fouling than stacks with spacers.

The charge of the membranes does strongly influence the rate and the type of fouling. At the anion exchange membranes, remnants of diatoms, clay minerals and organic fouling are observed. At cation exchange membranes, scaling of calciumphosphate is observed. Plastic sheets of non-conductive PE are least sensitive to fouling.

The decrease in obtained power density in the first day of the experiment is, most likely, caused by organic fouling. Several strategies are proposed to reduce this fouling, such as periodical switching of the current direction by means of switching the feed waters, to remain a high power density in RED.

Acknowledgments

This research is performed at Wetsus, Technological Top Institute for Water technology. Wetsus is funded by the Dutch Ministry of Economic Affairs, the European Union Regional Development Fund, the Province of Fryslân, the City of Leeuwarden and the EZ/Kompas program of the 'Samenwerkingsverband Noord-Nederland'. The authors are thankful for the support of the participants of the research theme 'Blue Energy'. In addition, the authors thank Arie Zwijnenburg for obtaining SEM and EDX results, Sjoerd Veldhuis for obtaining the XRD results and Kamuran Yasadi, Urania Michaelidou and Jan Post for the fruitful discussions.

REFERENCES

Allison, R.P., 1995. Electrodialysis reversal in water reuse applications. Desalination 103 (1–2), 11–18.

Blel, W., Legentilhomme, P., Bénézech, T., Legrand, J., Le Gentil-Lelièvre, C., 2009. Application of turbulent pulsating flows to the bacterial removal during a cleaning in place procedure. Part 2: effects on cleaning efficiency. Journal of Food Engineering 90 (4), 433–440.

Cifuentes-Araya, N., Pourcelly, G., Bazinet, L., 2011. Impact of pulsed electric field on electrodialysis process performance and membrane fouling during consecutive demineralization of a model salt solution containing a high magnesium/calcium ratio. Journal of Colloid and Interface Science 361 (1), 79–89.

Długołęcki, P.E., Nijmeijer, K., Metz, S.J., Wessling, M., 2008. Current status of ion exchange membranes for power generation from salinity gradients. Journal of Membrane Science 319 (1–2), 214–222.

EIA, 2010. International Energy Outlook 2010. U.S. Department of Energy, Washington D.C.

Grebenyuk, V.D., Chebotareva, R.D., Peters, S., Linkov, V., 1998. Surface modification of anion-exchange electrodialysis membranes to enhance anti-fouling characteristics. Desalination 115 (3), 313–329.

Grebenyuk, V.D., Grebenyuk, O.V., 2002. Electrodialysis: from an idea to realization. Russian Journal of Electrochemistry 38 (8), 806–809.

Katz, W.E., 1979. The electrodialysis reversal (EDR) process. Desalination 28, 31–40.

Kim, T., Kang, J., Lee, J.-H., Yoon, J., 2011. Influence of attached bacteria and biofilm on double-layer capacitance during biofilm monitoring by electrochemical impedance spectroscopy. Water Research 45 (15), 4615–4622.

Kjelstrup Ratjke, S., Fiksdal, L., Holt, T., 1984. Effect of Biofilm Formation on Salinity Power Plant Output on Laboratory Scale. University of Trondheim, Trondheim, p. 14.

Korngold, E., de Körösy, F., Rahav, R., Taboch, M.F., 1970. Fouling of anionselective membranes in electrodialysis. Desalination 8 (2), 195–220.

Lacey, R.E., 1980. Energy by reverse electrodialysis. Ocean Engineering 7 (1), 1–47.

Lee, H.-J., Moon, S.-H., Tsai, S.-P., 2002. Effects of pulsed electric fields on membrane fouling in electrodialysis of NaCl solution containing humate. Separation and Purification Technology 27 (2), 89–95.

Lindstrand, V., Jönsson, A.-S., Sundström, G., 2000a. Organic fouling of electrodialysis membranes with and without applied voltage. Desalination 130 (1), 73–84.

Lindstrand, V., Sundström, G., Jönsson, A.-S., 2000b. Fouling of electrodialysis membranes by organic substances. Desalination 128 (1), 91–102.

Norman, R.S., 1974. Water salination: a source of energy. Science 186 (4161), 350–352.

Post, J.W., Veerman, J., Hamelers, H.V.M., Euverink, G.J.W., Metz, S.J., Nijmeijer, K., Buisman, C.J.N., 2007. Salinity-gradient power: evaluation of pressure-retarded osmosis and reverse electrodialysis. Journal of Membrane Science 288 (1–2), 218–230.

Post, J.W., 2009. Blue energy: electricity production from salinity gradients by reverse electrodialysis. PhD thesis, Wageningen University.

Post, J.W., Hamelers, H.V.M., Buisman, C.J.N., 2009. Influence of multivalent ions on power production from mixing salt and

fresh water with a reverse electrodialysis system. Journal of Membrane Science 330 (1–2), 65–72.
Ramon, G.Z., Feinberg, B.J., Hoek, E.M.V., 2011. Membrane-based production of salinity-gradient power. Energy & Environmental Science 4 (11), 4423–4434.
RRUFF, 2012. Database of Raman Spectra, X-ray Diffraction and Chemistry Data for Minerals.
She, Q., Jin, X., Li, Q., Tang, C.Y., 2012. Relating reverse and forward solute diffusion to membrane fouling in osmotically driven membrane processes. Water Research 46 (7), 2478–2486.
Sumper, M., 2002. A phase separation model for the nanopatterning of diatom biosilica. Science 295 (5564), 2430–2433.
Vermaas, D.A., Saakes, M., Nijmeijer, K., 2011a. Double power densities from salinity gradients at reduced intermembrane distance. Environmental Science and Technology 45 (16), 7089–7095.
Vermaas, D.A., Saakes, M., Nijmeijer, K., 2011b. Power generation using profiled membranes in reverse electrodialysis. Journal of Membrane Science 385–386 (0), 234–242.
Vermaas, D.A., Guler, E., Saakes, M., Nijmeijer, K., 2012. Theoretical power density from salinity gradients using reverse electrodialysis. Energy Procedia 20, 170–184.
Vrouwenvelder, J.S., Schulenburg, D.A.G.V.D., Kruithof, J.C., Johns, M.L., Loosdrecht, M.C.M.v, 2009. Biofouling of spiral-wound nanofiltration and reverse osmosis membranes: a feed spacer problem. Water Research 43 (3), 583–594.
Wick, G.L., 1978. Power from salinity gradients. Energy 3 (1), 95–100.
Yip, N.Y., Tiraferri, A., Phillip, W.A., Schiffman, J.D., Hoover, L.A., Kim, Y.C., Elimelech, M., 2011. Thin-film composite pressure retarded osmosis membranes for sustainable power generation from salinity gradients. Environmental Science & Technology 45 (10), 4360–4369.